JOURNAL OF EXPERIMENTAL AND THEORETICAL PHYSICS, 2024, Vol. 165, No. 1, pp. 93–108

DYNAMIC AND STATIC PROPERTIES OF A NON-HEISENBERG ANISOTROPIC ANTIFERROMAGNET AT NON-ZERO TEMPERATURE

© 2024 E. A. Yarygina, V. V. Kozachek, Ya. Yu. Matyunina, O. A. Kosmachev, Yu. A. Fridman*

Vernadsky Crimean Federal University, Simferopol, 295007, Russia

e-mail: yuriifridman@gmail.com

Received July 22, 2023
Revised August 31, 2023
Accepted August 31, 2023

Abstract. In the mean-field approximation, the influence of both temperature and single-ion easy-axis anisotropy on the phase states and excitation spectra of a non-Heisenberg antiferromagnet with S = 1 is studied. The temperature dependences of vector and tensor order parameters are determined both in phases with vector and tensor order parameters. The dependence of excitation spectra on temperature and anisotropy constant has been studied. It is shown that at temperatures other than zero, an additional (non-relaxation) branch of excitations arises. The temperature dependence of the phase diagram has been studied.

Keywords: *temperature, antiferromagnet, "easy plane" anisotropy, non-Heisenberg exchange interaction*

DOI: 10.31857/S00444510240110e4

1. INTRODUCTION

In modern microelectronics and spintronics devices, magnetic materials with a compensated magnetic moment are actively used, i.e. magnets with antiferromagnetic ordering [1]. This choice is due to the fact that an exchange gain effect is observed in antiferromagnets, which significantly increases the frequency of antiferromagnetic resonance to the terahertz range, and also significantly enhances other dynamic characteristics of the system, such as the limiting velocities of domain walls [2] and magnetic vortices [3, 4]. Also, the spin current significantly affects the properties of compensated magnets [5-12], and it is this circumstance that makes them so attractive for use in spintronics. At the same time, one of the "hottest" topics of the physics of magnetism is the search for new phase states of magnetically ordered systems.

The standard magnetic ordering is characterized by a vector parameter of the order (average value of the $\langle S_n \rangle$ spin at the node) [13-15], non- invariant with respect to time reversal. However, besides the standard magnetic order (ferro- or antiferromagnetic), there are systems such as rare earth dielectrics [16], iron-based superconductors [17-21] and a number of others, in which magnetic ordering is more complex than the standard one. This ordering includes nematic [14, 15, 22-33]. This state is similar to ordering in liquid crystals [34], whence in fact the name "spinous nematicus" was derived. Spin nematic states are found in $LiCuVO_4$ magnets [33, 35, 36], rare-earth magnets [37] and low-dimensional systems (see, for example, [30]).

In a magnet with S = 1, taking into account a large biquadratic exchange interaction of the form $K(S_n S_{n'})^2$ leads to the realization of a spin nematic state [38]. The spin nematic is characterized by a spontaneous violation of rotational symmetry, which is associated with spin quadrupole parameters see [26-32]. Note that the quadrupole averages characterizing the

$$Q_{\alpha\beta} = \left\langle S^{\alpha} S^{\beta} + S^{\beta} S^{\alpha} \right\rangle - \frac{1}{3}\delta_{\alpha\beta} S(S+1),$$
$$\alpha, \beta = x, y, z,$$

nematic state are invariant relative to time reversal. The geometric image of these averages is a quadrupole ellipsoid with axes e_1, e_2 and e_3, chosen in such a way that $\langle S_\alpha S_\beta + S_\beta S_\alpha \rangle = 0$ at $\alpha \neq \beta$, $\alpha, \beta = 1,2,3$, and the semi-axes of the latter are equal to $\langle S_1^2 \rangle, \langle S_2^2 \rangle$ and $\langle S_3^2 \rangle$. At zero temperature T = 0, the quadrangular ellipsoid degenerates into a flat disk, $\langle S_1^2 \rangle = \langle S_2^2 \rangle = 1, \langle S_3^2 \rangle = 0$. At a temperature different from zero, but lower than the critical temperature $T < T_c$, the value is $0 < \langle S_3^2 \rangle < \langle S_{1,2}^2 \rangle$, when $T > T_c$ the rotational symmetry is restored $Q_{\alpha\beta}$ [22, 39–42].

Due to the isotropy of the exchange interaction, the direction of the quantization axis z is arbitrary, the state of the spin nematic can be described by introducing a vector-director n, which is directed along the axis of rotation of a quadrupole ellipsoid. It is understood that the states with **n** and **-n** are indistinguishable, and the value $Q_{\alpha\beta}$ is a quantum analogue of the De Gennes order parameter, which is introduced for ordinary nematic liquid crystals [34].

In the case when the exchange integral $J < 0$ is negative, states with two magnetic sublattices arise for a crystalline magnet. If the Heisenberg exchange exceeds the bi-quadratic one, then the usual antiferromagnetic state is realized in the magnet. In the opposite case, the situation is more interesting and the question of the basic state is not trivial, since the states with **n** and **-n** are identical. Within the framework of the mean field approximation, it can be shown that the system implements the state of an orthogonal nematic, for which the directions n are orthogonal in two sublattices [25, 26, 43]. Since there are three such directions of vector n, in the one-dimensional case this state is defined as not fully ordered (semiordered) [25], although the stability of the two-lattice phase within the framework of the mean field approximation is proved for a square lattice [26], and a three-lattice one for the triangular lattice [27, 28], see Fig. 1, 2 in [28]. The orthogonal nematic-ferromagnetic and orthogonal nematic-antiferromagnetic phase transitions occurring with a change in the J/K parameter are degenerate transitions of the first kind [26].

Most studies of spin nematics were limited to the case of low temperatures when considering the isotropic model [26-32], or a model taking into account the one-ionic anisotropy [43-45]. As it was shown in [43], the influence of a single-ionic anisotropy of the type "light axis" leads to significant changes in the dynamics of the spin nematic even at T = 0, although it does not change the phase pattern compared with the isotropic case. The influence of temperature, i.e. thermal fluctuations, on the properties of spin nematic has not been sufficiently studied [40, 46-49]. In [47, 48], the influence of the temperature on the behavior of both the order parameters and the excitation spectra of a magnet with large single-ion anisotropy, comparable or even exceeding the constant of the bilinear exchange interaction. However, these models do not describe the state of the spin nematic. In this regard, it is of interest to study the effect of both single-ionic anisotropy of the type "light axis" and temperature on the behavior of order parameters and excitation spectra at different ratios of the material parameters of the system.

2. MODEL AND BASIC CONDITIONS

As a model, let us consider a non-Heisenberg antiferromagnet, in which, in addition to the bilinear exchange interaction, the bi-quadratic exchange interaction is taken into account, as well as one-ionic anisotropy of the type "light axis". The spin of the magnetic ion is S = 1. The Hamiltonian of such a model can be represented as

$$\mathcal{H} = -\frac{1}{2}\sum_{n,n'}\left[J\left(n\text{–}n'\right)\left(S_n\cdot S_{n'}\right)+K\left(n\text{–}n'\right)\left(S_n S_{n'}\right)^2\right]- -\frac{D}{2}\sum_n\left(S_n^z\right)^2, \quad (1)$$

where S_n is the spin operator at the n-th node, J, K are the constants of bilinear and biquadratic exchange interactions, respectively, D > 0 is a constant of one- ionic anisotropy of the type "light axis". We will limit ourselves to considering lattices that allow splitting into two equivalent sublattices, for example, cubic or square. Previously, similar models were considered only when T = 0. It was shown in [26, 43] that in a non-Heisenberg magnet with S = 1 at T = 0 , it is possible to realize four phase states: the ferromagnetic phase with a predominant bilinear exchange interaction (J > K), at J < 0 and | J | > K an antiferromagnetic state is realized, but if J > 0,K > 0 and J < K, the nematic phase is stable in the system, and finally, if J < 0, K < 0 and | J |<| K |, then the orthogonal-nematic phase is realized.

Let us consider the behavior of the system described by the Hamiltonian (1) at a temperature other than zero, but not exceeding the critical temperature. Using a diagrammatic technique for Hubbard operators [26, 44, 45, 50-52], let's determine the energy levels of the magnetic ion

$$E_{1,-1} = -\frac{D}{2} \mp \overline{H}\cos 2\theta - B_2^0 \mp B_2^2 \sin 2\theta, \quad E_0 = 2B_2^0, \quad (2)$$

where

$$\overline{H} = \left(J_0 - \frac{K_0}{2}\right)\left\langle S^z\right\rangle,$$

$$B_2^0 = \frac{K_0}{6}q_2^0, \quad B_2^2 = \frac{K_0}{2}q_2^2,$$

$$\varepsilon = \frac{1}{2}\left(J_0 - \frac{K_0}{2}\right)\left\langle S^z\right\rangle^2 + \frac{K_0}{12}\left(q_2^0\right)^2 + \frac{K_0}{4}\left(q_2^2\right)^2,$$

ε is an additive constant independent of spin operators,

$$q_2^0 = 3\left\langle \left(S^z\right)^2 \right\rangle - 2, \quad q_2^2 = \left\langle \left(S^x\right)^2 \right\rangle - \left\langle \left(S^y\right)^2 \right\rangle$$

are components of the quadrupole moment tensor.

Using the connection of spin operators with Hubbard operators [26, 46, 53, 54]

$$S_n^z = \cos 2\theta \left(X_n^{11} - X_n^{-1-1} \right) - \sin 2\theta \left(X_n^{1-1} + X_n^{-11} \right),$$

$$S_n^+ = \sqrt{2} \left[\sin\theta \left(X_n^{01} - X_n^{-10} \right) + \cos\theta \left(X_n^{10} + X_n^{0-1} \right) \right],$$

$$S_n^- = \left(S_n^+ \right)^+,$$

it is possible to determine the dependence of vector and tensor order parameters on both temperature and material parameters of the system, i.e. on the magnitude of exchange integrals and the anisotropy constant:

$$\left\langle S^z \right\rangle = \cos 2\theta \frac{\exp\left(-E_1 / T\right) - \exp\left(-E_{-1} / T\right)}{Z}, \qquad (3)$$

$$q_2^0 = 3\frac{\exp\left(-E_1 / T\right) + \exp\left(-E_{-1} / T\right)}{Z} - 2, \qquad (4)$$

$$q_2^2 = \sin 2\theta \frac{\left(\exp - E_1 / T\right) - \exp\left(-E_{-1} / T\right)}{Z}, \qquad (5)$$

B (3)–(5) Z is the statistical sum, which in this case is equal to

$$Z = \sum_{M=-1,0,1} \exp\left(-\frac{E_M}{T} \right) =$$
$$= \exp\left(\frac{-E_1}{T} \right) + \exp\left(\frac{-E_0}{T} \right) + \exp\left(\frac{-E_{-1}}{T} \right),$$

E_M stands for the energy levels of the magnetic ion, determined by expressions (2). Also in formulas (3)-(5) and the expression for the statistical sum, the Boltzmann constant is equal to one, and the temperature is measured in units of energy. θ is the parameter of the Bogolyubov *u-v* transformation [47], determined by the ratio

$$\bar{H} \sin 2\theta = B_2^2 \cos 2\theta.$$

Note that the parameter θ clearly does not depend on the constant of single-ionic anisotropy, but depends both on the constants of exchange interactions and parameters of the order $\left\langle S^z \right\rangle$ and q_2^2.

3. ORDER PARAMETERS OF THE NON-HEISENBERG ANTIFERROMAGNET

3.1 Ferromagnetic phase

As shown in [26, 43], in the case of low temperatures and predominant bilinear exchange interaction (J > K), the parameter θ is zero (θ = 0). Taking this into account, as well as the fact that the lowest energy level of the magnetic ion at $T \to 0$ is E_1, it follows from the ratios (3)–(5)

$$\left\langle S^z \right\rangle = 1, \quad q_2^0 = 1, q_2^2 = 0.$$

These values of the order parameters indicate that at J > K and θ = 0, the ferromagnetic phase (FM) is formed in the system. Numerical analysis of the system of equations (3)–(5) allows us to determine the effect of thermal fluctuations on the behavior of the system parameters in the FM phase. Figures 1 *a*, *b*, *c* show these results for the FM phase at different values of the single-ionic anisotropy constant.

All variables in Figure 1 are given in relative units (D/J, T/J). As can be seen in Fig. 1 a, b, c, the average value of the magnetic moment (per node) decreases with increasing temperature, this is due to the increase in thermal fluctuations. Turning the average magnetic moment to zero makes it possible to determine the Curie temperature (see Fig. 1 a, b, c), which increases with the growth of the one-ion anisotropy constant. This is easy to understand if we remember that the magnetic moment in the ferromagnetic phase is oriented along the axis of light magnetization, and the greater the anisotropy constant, the more energy is necessary for the destruction of the vector magnetic order and therefore the higher is the critical temperature.

The analysis of equations (3)–(5) allows us to estimate the Curie temperature in the FM phase:

$$T_C = \left(J_0 - \frac{K_0}{2} \right) \frac{2 + q_2^0}{3}.$$

If we neglect the biquadratic exchange interaction, then this expression is for the Curie temperature corresponds to the standard result obtained in the mean field approximation [55]. In addition, it should be noted that the Curie temperature estimate we have obtained implicitly depends on the magnitude of the one-ionic anisotropy constant. As follows from (3)–(5), as well as Fig. 1 a, b, c, at temperatures close to T_C, the parameter q_2^0 the more strongly differs from zero, the greater the value of the single-ion anisotropy constant, since a large D value stabilizes the axis of the quadrupole ellipsoid.

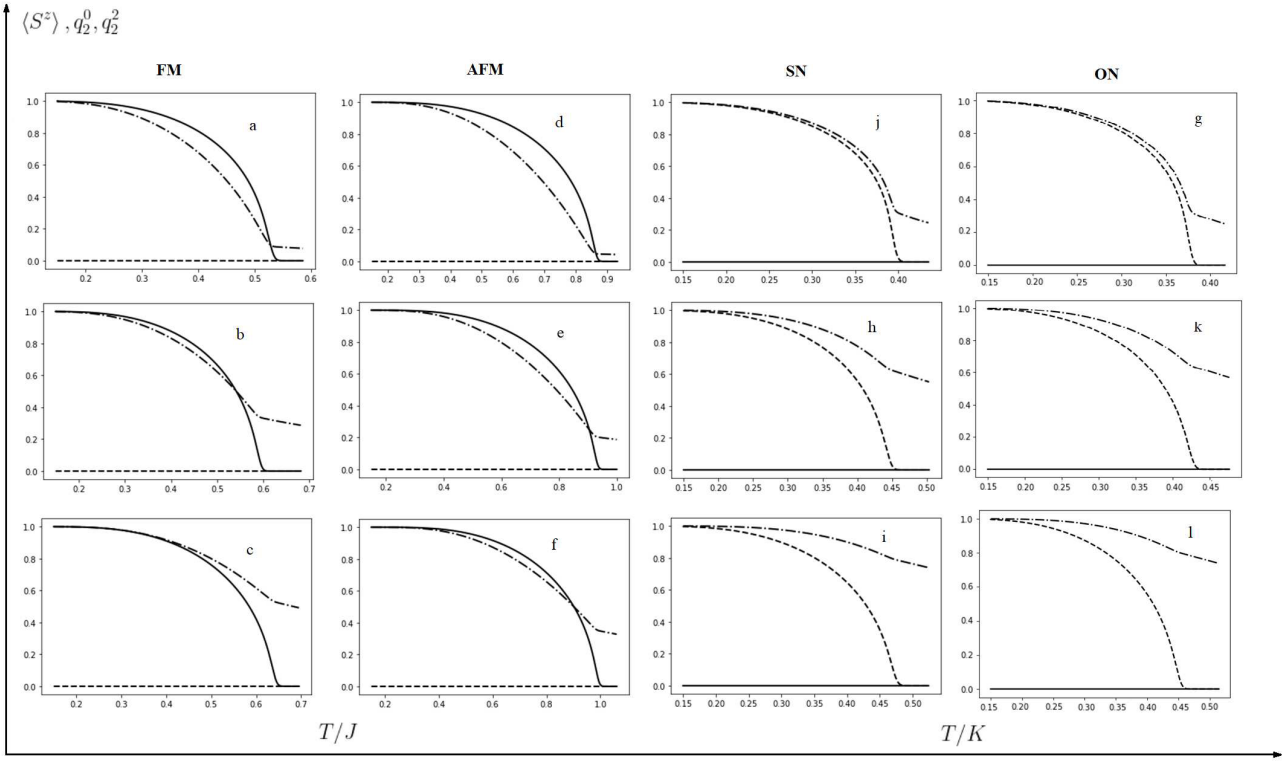

Fig. 1. Dependences of the order parameters of a non-Heisenberg anisotropic ferromagnet with S = 1 on temperature in various phases. *a-c* FM phase, exchange integrals J = 1, K = 0.5, *d-f* AFM phase, exchange integrals J = -1, K = 0.5, D/J = 0.1 (a, d), D/J = 0.5 (b, e), D/J = 1.0 (c, f). j-i SN-phase, exchange integrals J = 0.2, K = 1.0, g-l show ON-phase, exchange integrals J = -0.3, K = -1.9, D/K = 0.1 (j, g), D/K = 0.5 (h, k), D/K = 1.0 (i, l). Solid lines: $\langle S^z \rangle$, dashed lines q_2^2, dashed dotted lines q_2^0.

As for the behavior of tensor order parameters in the FM phase, it is quite expected: parameter $q_2^2 = 0$ in the entire temperature range, since in this phase

$$\left\langle \left(S^x\right)^2 \right\rangle = \left\langle \left(S^y\right)^2 \right\rangle,$$

and the parameter is q_2^0 is different from zero in the entire temperature range, since it is proportional to $\left\langle \left(S^z\right)^2 \right\rangle$ and does not depend on the orientation of the magnetic moment. At $T > T_C$, in the isotropic case, the rotational symmetry of the tensor is

$$Q_{\alpha\beta} = \frac{1}{2}\left\langle S^\alpha S^\beta + S^\beta S^\alpha \right\rangle$$

restored, i.e.

$$\left\langle \left(S^x\right)^2 \right\rangle = \left\langle \left(S^y\right)^2 \right\rangle = \left\langle \left(S^z\right)^2 \right\rangle = \frac{2}{3}.$$

However, as can be seen in Fig. 1 a, b, c, the presence of single-ion anisotropy of the "light axis" type leads to the fact that the component of the quadrupole tensor q_2^0 significantly depends on the value of the anisotropy constant, which violates the rotational symmetry of the $Q_{\alpha\beta}$ tensor at $T > T_C$.

3.2 The nematic phase

Let us now consider the situation when the biquadratic exchange interaction is predominant, i.e. when the parameter θ in this case is equal to π / 4 [26, 43]. In addition, in this case, at $T \to 0$, the state of spin nematic (SN) is realized in the magnet, which is characterized by the following parameters of the order:

$$\left\langle S^z \right\rangle = 0, q_2^0 = 1, q_2^2 = 1.$$

The geometric image of this state when at low temperatures is a uniaxial ellipsoid with semi-axes

$$\left\langle \left(S^z\right)^2 \right\rangle = 1, \left\langle \left(S^x\right)^2 \right\rangle = 1,$$

$$\left\langle \left(S^y\right)^2 \right\rangle = 0,$$

i.e. an infinitely thin disk lying in the zx plane. The vector director is perpendicular to the plane of the disk, i.e. directed along the y axis.

The behavior of the parameters of the order of a non-Heisenberg ferromagnetic with S = 1 as functions of temperature and anisotropy constant is shown in Fig. 1 j, h, i. As can be seen in Fig. 1 j, h, i, with increasing temperature, the quadrupole parameter q_2^2 becomes less than one. This means that $\left\langle \left(S^y\right)^2 \right\rangle \neq 0$ and, therefore, the quadrupole ellipsoid becomes biaxial, and its orientation is determined by the axis of anisotropy.

As the numerical analysis of the equations (3)–(5) shows, given in Fig. 1 j, h, i, the average value of the magnetic moment (per node) in the SN phase is zero over the entire temperature range and at any values of the anisotropy constant. AS far as the tensor parameters of the order are concerned, the component of the quadrupole moment tensor

$$q_2^2 = \left\langle \left(S^x\right)^2 \right\rangle - \left\langle \left(S^y\right)^2 \right\rangle$$

is zero at temperature T_Q, which determines the temperature of the phase transition from the SN phase to the paramagnetic one. It should be noted that this temperature increases with the growth of the one-ionic anisotropy constant (although this growth is not as significant as during the FM-phase–paramagnetic phase transition). Temperature dependence of the parameter of the order q_2^0 shows that at $T > T_Q$, the rotational symmetry of the $Q_{\alpha\beta}$ tensor is violated, which is associated with the presence of anisotropy of the "light axis" type. In addition, using the ratio (3)-(5), in the approximation of the mean field, we estimated the transition temperature (T_Q)from the spin nematic state to the paramagnetic phase:

$$T_Q = \frac{K_0}{2}\frac{2+q_2^0}{3}.$$

As you can see, this temperature, as expected, is determined only by the biquadratic exchange interaction and tensor parameters of the order.

3.3 Antiferromagnetic phase

Let us now consider a situation in which the constants of exchange interactions are related by the ratio |J| > K, where J < 0, K > 0. In this case, it is energetically advantageous for the system to split into two equivalent sublattices, i.e., to switch to the antiferromagnetic state (AFM). As shown in [26, 43], at $T \to 0$, the u-v transformation parameter takes the values $\theta_1 = 0$ and $\theta_2 = \pi / 2$ for the first and second sublattices, respectively. The order parameters of the first and second sublattices at T = 0 have the form [43]

$$\left\langle S_1^z \right\rangle = \left| \left\langle S_2^z \right\rangle \right| = 1, q_{2(1)}^0 = q_{2(2)}^0 = 1, q_{2(1)}^2 = q_{2(2)}^2 = 0.$$

It is taken into account here that the magnetizations of the first and second sublattices are antiparallel. It is of interest to investigate the behavior of the parameters of the sequence at arbitrary temperatures in the AFM phase using the ratios (3)–(5). At the same time, it is enough to consider one sublattice, since they are equivalent. A numerical analysis of the dependence of the parameters of the order of a non-Heisenberg easy-plane magnet on temperature and the value of the anisotropy constant in the AFM phase is given in Fig. 1 d, e, f.

It follows from Fig. 1 d, e, f that the behavior of the average value of the magnetic moment (per node) is analogous to its behavior in the FM phase, i.e., with an increase in temperature, it decreases, which is associated with the influence of thermal fluctuations. Just as in the FM phase, turning the average magnetic moment to zero makes it possible to determine the Neel temperature. However, as can be seen in Fig. 1 j, h, i and Fig. 1 d, e, f, the Neel temperature is significantly higher than the Curie temperature and increases with an increase in the one-ion anisotropy constant. The dependence of the Neel temperature on the anisotropy constant is easy to understand if we recall that the magnetic moment of the sublattice in the AFM phase is parallel to the axis of light magnetization, and the greater the anisotropy constant, the more energy is needed to destroy the vector magnetic order, and consequently, the higher the critical temperature. More interesting is the question of the growth of the Neel temperature in comparison with the Curie temperature at the same values of the anisotropy constant. So, if we do not take into account the biquadratic exchange interaction (Heisenberg magnet), then the Curie and Neel temperatures do not coincide, and correspond to the standard result obtained in the mean field approximation [47]. When biquadratic exchange interaction is enabled, the situation changes. So, when J > K > 0 the bilinear exchange interaction tends to establish a ferromagnetic ordering, and the biquadratic one is quasi-antiferromagnetic. Such competition leads to a decrease in the Curie temperature (see the expression for T_C in the

FM phase). In the AFM phase (at J < 0,K > 0, |J| > K) both bilinear exchange interaction and biquadratic interaction tend to establish antiferromagnetic ordering. This circumstance leads to an increase in the Neel temperature compared to the Curie temperature. In addition, the analysis of equations (3)-(5) makes it possible to estimate the Neel temperature in the AFM phase:

$$T_N = \left(|J_0| + \frac{K_0}{2}\right)\frac{2+q_2^0}{3}.$$

As for the temperature dependence of the tensor order parameters in the AFM phase, it is analogous to their behavior in the FM phase.

3.4 Orthogonal-nematic phase

If the exchange interaction constants are related by the ratio J < 0,K < 0, |J| < |K|, then splitting into two sublattices is advantageous for the magnet. However, the ordering in this case is not antiferromagnetic but orthogonal-nematic (ON) [26, 56]. This state can be considered as a nematic state in each of the sublattices, but the state vectors of the sublattices are orthogonal (for more details, see [26]). At T = 0, the parameters of the ON-phase sequence are equal to

$$\left\langle S_1^z\right\rangle = \left\langle S_2^z\right\rangle = 0, q_{2(1)}^0 = q_{2(2)}^0 = 1,$$
$$q_{2(1)}^2 = -q_{2(2)}^2 = 1.$$

In the case of temperatures other than zero, the behavior of the order parameters is determined by the correlations (3)-(5). Numerical analysis of these correlations allows us to determine the dependence of the order parameters on both temperature and the value of the single-ion anisotropy constant. The results of such an analysis are shown in Fig. 1 g, k, l. At the same time, it is taken into account that the sublattices are equivalent and it is sufficient to consider the behavior of one of the sublattices.

As follows from our analysis of relations (3)-(5), the orthogonal-nematic state is preserved throughout the temperature range (excluding the fluctuation region), i.e.

$$\left\langle S_i^z\right\rangle = 0, \quad i = 1,2,$$

and the behavior of tensor parameters of the order q_2^0, q_2^2 is similar to their behavior in the SN phase. It should be noted that the conversion to zero of the parameter q_2^2 allows estimating the transition temperature of the magnet from the orthogonal-nematic phase to the paramagnetic one. As can be seen from the comparison of Fig. 1 d, e, f and Fig. 1 g, k, l, this temperature (T_{Q1}) is significantly less than the temperature of the SN-phase– paramagnetic phase transition. When describing both AFM and ON phases we used extended zone schemes. In this case, it turns out that this representation is quite convenient and visual, since the sub- lattices are equivalent. In this scheme, it is necessary to change the constant of the biquadratic exchange action in the energy levels of the magnetic ion (2)

$$K \to -\frac{K}{2} = \frac{|K|}{2}.$$

Then an analytical estimate of the temperature in the transition ON-phase–the paramagnetic phase has the form

$$T_{Q1} = \frac{|K_0|}{4}\frac{2+q_2^0}{3}.$$

Thus, both numerical analysis and analytical estimation have shown that temperature T_{Q1} is significantly less than temperature T_Q.

4. DYNAMICS OF THE SPIN NEMATIC AT ARBITRARY TEMPERATURES

We investigate the behavior of the spectra of elementary excitations of the system under consideration at temperatures other than zero. The excitation spectra are determined by the poles of the Green's function [44, 45, 47, 49, 51, 52], which, within the framework of the Hubbard's operators technique is defined as follows [32, 46, 49, 51, 52]:

$$G^{\lambda\lambda'}(n,\tau,n',\tau') = -\left\langle \hat{T}\tilde{X}_n^{\lambda}(\tau)\tilde{X}_{n'}^{\lambda'}(\tau')\right\rangle,$$

where

$$\tilde{X}_n^{\lambda}(\tau) = \exp(H\tau)X_n^{\lambda}\exp(-H\tau)$$

is the Hubbard operator in the Heisenberg representation, $\hat{T}$ is the Wick operator, λ are root vectors defined by the algebra of Hubbard operators [44, 47]. The derivation of the dispersion equation is described in detail in the works [39, 44, 46, 51, 52], therefore, here we give only the form of this equation

$$\det\left\|\delta_{ij} + x_{ij}\right\| = 0, \quad i,j = 1,2,...,8, \tag{6}$$

$$x_{ij} = G_0^{\alpha}(\omega_n)b(\alpha)c_{ij}(\alpha),$$

where

$$G_0^{\alpha}(\omega_n) = \left[i\omega_n + \alpha E\right]^{-1}$$

is Green's zero function,

$$c_{ij}(\alpha,\beta) = a_{ik}(\alpha,\beta)A_{kj},$$

$$a_{ik}(\alpha,\beta) = c_i(\alpha)c_k(-\beta).$$

The components of the vector $c(\lambda)$ are determined from the connection of spin operators with Hubbard operators, and the matrix $\hat{A}_{nn'}$ can be represented as

$$\hat{A}_{n_1n_2} = \hat{A}^3_{n_1n_2} \oplus \hat{A}^5_{n_1n_2},$$

$b(\alpha) = \langle \alpha \mathbf{X} \rangle$ are terminal factors, with the decisive one that can be explicitly represented as [51, 55]

$$b(\alpha_1) = -b(\alpha_2) = \frac{-\exp(-E_1 / T) + \exp(-E_0 / T)}{Z},$$

$$b(\alpha_3) = -b(\alpha_4) = \frac{\exp(-E_1 / T) - \exp(-E_{-1} / T)}{Z}, \quad (7)$$

$$b(\alpha_5) = -b(\alpha_6) = \frac{\exp(-E_0 / T) - \exp(-E_{-1} / T)}{Z}.$$

where E_i are the energy levels of the magnetic ion (i = 1, 0,-1), determined by the relations (2), and α_i root vectors (i = 1, ..., 6), the components of which are determined by the algebra of Hubbard operators [39], and in this case are equal to:

$$\alpha_1 = \alpha(0,1) = (-1,1,0), \alpha_2 = \alpha(1,0) = (1,-1,0),$$

$$\alpha_3 = \alpha(1,-1) = (1,0,-1), \alpha_4 = \alpha(-1,1) = (-1,0,1),$$

$$\alpha_5 = \alpha(0,-1) = (0,1,-1), \alpha_6 = \alpha(-1,0) = (0,-1,1).$$

It should be noted that the dispersion equation (6), which determines the excitation spectra, is valid for an arbitrary ratio of material constants, i. e. various phase states and the temperature range of the magnet's order existence (excluding the fluctuation area).

In [32-36, 53], the solutions of the dispersion equation (6) at T = 0 were studied in detail both for an isotropic spin nematic with S = 1 and for a non-Heisenberg magnet with uniaxial anisotropy. It was shown that at T = 0, two branches of elementary excitations are realized in the magnet, one of which is precession and is associated with the

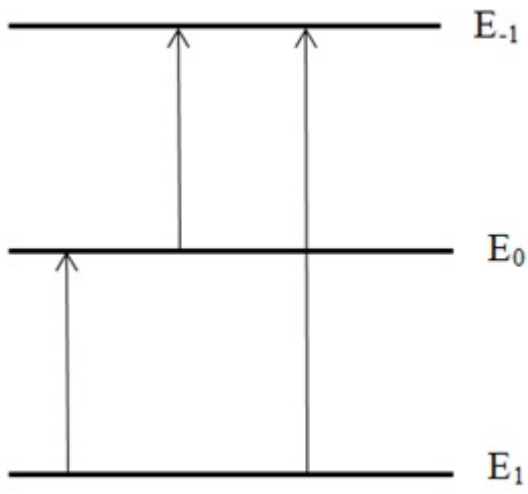

Fig. 2. The energy levels of the magnetic ion and the transitions between them.

transition of the magnetic ion from the basic state (E_1) to the first non-excited state (E_0), i.e. in this mode, the alternating spin density fluctuations are associated with turns of the directions of the main axis of the quadrupole ellipsoid. The second branch of excitations is associated with the transition of the magnetic ion from the ground state E_1 to the state E_{-1}. This mode includes longitudinal fluctuations of the modulus of the magnetization vector, the direction of which remains parallel to the main axis of the ellipsoid of quadrupole moments, deformation of the ellipsoid and its rotation around the magnetization, i.e. this mode is a longitudinal branch of the oscillations. It should be noted that in an isotropic non-Heisenberg magnet with S = 1 in the non- magnetic phase, both branches of excitations coincide (see [26]). In addition to these excitation branches, another branch associated with the excited states of the magnetic ion $E_0 \to E_{-1}$ is realized in the model studied here (see Fig. 2), i.e., the temperature "thaws" the degree of freedom of the magnetic field ion. Moreover, the excitation branch associated with the transition of the magnetic ion E_{0-1} is not a relaxation one. We study in more detail the excitation spectra of the non-Heisenberg anisotropic antiferromagnetic at different ratios of exchange integrals.

4.1 Excitation spectra in the FM phase at $T \neq 0$

As noted earlier, the FM phase is implemented in the system under consideration at J > K and $T < T_C$. Let's consider the solutions of the dispersion equation (6) in this state.

At nonzero temperatures, this equation defines three branches of spin disturbances, two of which can be conditionally called "transversal", since they are associated with vibrations of a quadrupole ellipsoid, and one "longitudinal", associated with an oscillation of the magnetic moment modulus (quantum spin contraction). The explicit form of the spectra of these excitations has the form

$$\varepsilon_1^{\parallel}(k) = -E_{1-1} - K(k)b(\alpha_3), \tag{8}$$

$$\varepsilon_{2,3}^{\perp} = \frac{1}{2}\Big[E_{10} + E_{0-1} + J(k)\big(b(\alpha_2) + b(\alpha_5)\big)\Big] \pm \pm\frac{1}{2}\left\{\begin{array}{c}\Big[E_{10} - E_{0-1} + J(k)\big(b(\alpha_2) - b(\alpha_5)\big)\Big]^2 + \\ +4b(\alpha_2)b(\alpha_5)\big(J(k) - K(k)\big)^2\end{array}\right\}^{1/2}. \tag{9}$$

In (8) and (9) E_{ij} — is the difference in the energy levels of the magnetic ion (see expressions (2)), $b(\alpha_i)$ are the end multipliers determined by the ratios (7).

Given the explicit form of energy levels the magnetic ion in the FM phase and the terminal multipliers, as well as the fact that in this case the u-v transformation parameter $\theta = 0$, the spectra (8) and (9) can be represented in a more compact form:

$$\varepsilon_1^{\parallel}(k) = \big(2J_0 - K_0 - K(k)\big)\big\langle S^z\big\rangle, \tag{10}$$

$$\varepsilon_{2,3}^{\perp}(k) = \frac{1}{2}\big(2J_0 - K_0 - J(k)\big)\big\langle S^z\big\rangle \pm \pm\frac{1}{2}\left\{\begin{array}{c}\big(J(k) - K(k)\big)^2\Big[\big\langle S^z\big\rangle^2 - (q_2^0)^2\Big] + \\ +\Big(D - \big(J(k) - K(k)\big)q_2^0\Big)^2\end{array}\right\}^{1/2}. \tag{11}$$

In addition, when obtaining expressions (10) and (11), it was taken into account that in the FM phase

$$b(\alpha_3) = \big\langle S^z\big\rangle,$$

as well as

$$q_2^0 = 3\big\langle (S^z)^2\big\rangle - 2.$$

The temperature dependence of the spectra of elementary excitations in the FM phase is determined by dependence on the temperature of the average magnetic moment $\big\langle S^z\big\rangle$ and the components of the quadrupole moment tensor q_2^0 (see expressions (3)–(5)).

Let us consider the behavior of magnon spectra at different values of the one-ionic anisotropy constant and at nonzero temperatures. Note that the temperatures in question are significantly lower than the Curie temperature, which is due to the fact that the problem is considered in the approximation of the average.

First of all, let us consider the "longitudinal" branch of the excitations of $\varepsilon_1^{\parallel}$. As can be seen in Fig. 3 *a*–*d* and Fig. 3 *e*–*h*, and also based on formula (10), this branch depends on the wave vector as k^2, and this dependence varies slightly with changes in temperature and the constant of single-ion anisotropy. In addition, there is an energy gap in the spectrum of longitudinal magnons, which is clearly independent of the anisotropy $\big\langle S^z\big\rangle, q_2^0, q_2^2$ implicitly depend on the anisotropy constant:

$$\varepsilon_1^{\parallel}(0) = 2\big(J_0 - K_0\big)\big\langle S^z\big\rangle. \tag{12}$$

The behavior of the "transversal" branches of excitations is more complex. As follows from the correlations (9) and (11), these two branches are entangled, and the higher the temperature, the less pronounced this "entanglement". So, at a fairly low temperatures and low values of the anisotropy constant (see Fig. 3 a, b), the branches $\varepsilon_2^{\perp}$ and $\varepsilon_3^{\perp}$ practically merge into each other. This behavior is easy to understand if you pay attention to the behavior of the order parameters $\big\langle S^z\big\rangle$ and q_2^0 (see fig. 1 a, b, c). As follows from these graphs, at very low temperatures $t = 0.003$ and low anisotropy $d / j = 0.1$, the expression is

$$\big\langle S^z\big\rangle^2 - \big(q_2^0\big)^2 \to 0.$$

Then, as follows from (11), the "transversal" branch ε_2, at small wave vectors, behaves as follows:

$$\varepsilon_2^{\perp} = \alpha k^2 + D / 2,$$

and the second "transversal" branch is dispersionless:

$$\varepsilon_3^{\perp} = J_0 - K_0 - D / 2.$$

With the growth of the wave vector, the branches $\varepsilon_2^{\perp}$ and $\varepsilon_3^{\perp}$ merge into each other, i.e. at large k, the branch $\varepsilon_2^{\perp}$ becomes dispersionless, and $\varepsilon_3^{\perp}$ behaves like a quadratic parabola.

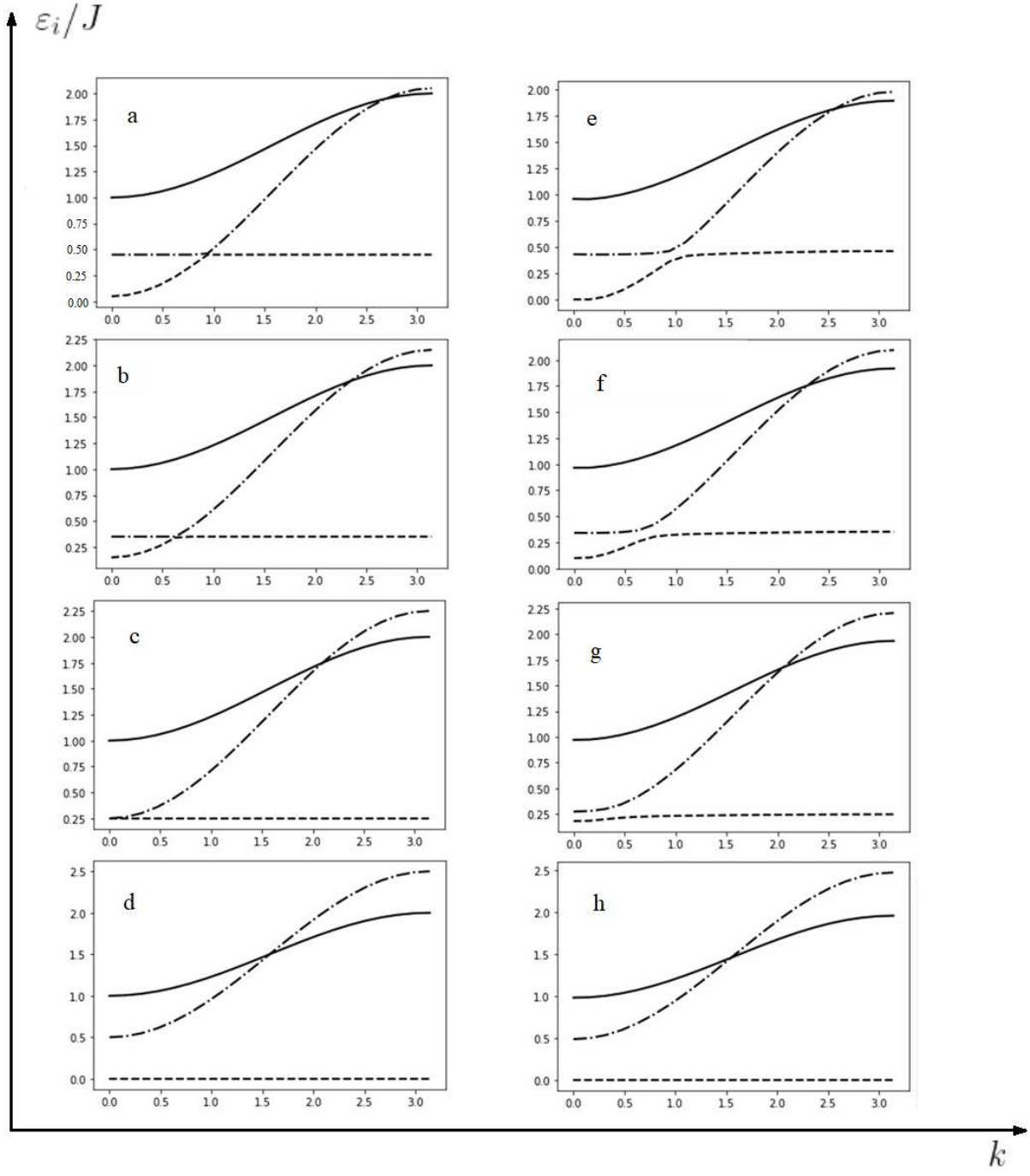

Fig. 3. Spectra of elementary excitations in the FM phase at $T / J = 0.003$ (*a*-*d*) and 0.3 (*e*-*h*) and anisotropy values $D / J = 0.1\,(a,e), 0.3\,(b,f), 0.5\,(c,g), 1.0\,(d,h)$. Solid lines correspond to the "longitudinal" branch of excitations $\varepsilon_2^{\perp} / J$, dashed lines correspond to the "transverse" branch $\varepsilon_2^{\perp} / J$, and the dotted line is a "transverse" branch $\varepsilon_3^{\perp} / J$, the exchange integrals J = 1, K = 0.5.

With an increase in temperature, for example at T/J = 0.3, as follows from Fig. 1 *a*, *b*, *c*, the value is

$$\left\langle S^z \right\rangle^2 - \left(q_2^0\right)^2 \neq 0.$$

This leads to the fact that the "transversal" branches begin to "push apart", and the higher the anisotropy of the magnet, the more active the pushing occurs. So, for D/J = 1, the "transverse" branch $\varepsilon_2^{\perp}$ becomes dispersionless, and the branch $\varepsilon_3^{\perp}$ behaves like k^2, moreover, the energy gap of this branch significantly depends on the value of the anisotropy constant (see Fig. 3).

4.2 Excitation spectra in the SN phase at $T \neq 0$

Let us now consider the behavior of the excitation spectra in the SN phase at different values of the anisotropy constant and arbitrary temperatures (excluding the fluctuation region). It is assumed that J < K, and the *u*-*v* conversion parameter θ in this case is equal to π/4. Taking into account that in this phase $\left\langle S^z \right\rangle = 0$, and q_2^2 coincides with the end factor $b(\alpha_3)$, the spectra of all three excitation branches can be represented as

$$\varepsilon_4^{\parallel}(k) = b(\alpha_3)\times \times\left\{\left(K_0 - K(k)\right)\left(K_0 + K(k) - 2J(k)\right)\right\}^{1/2}, \quad (13)$$

$$\varepsilon_5^{\perp}(k) = \left\{\left(\frac{D}{2} + b(\alpha_2)\left(K_0 - K(k)\right)\right)\times \times\left(\frac{D}{2} + b(\alpha_2)\left(K_0 + K(k) - 2J(k)\right)\right)\right\}^{1/2}, \quad (14)$$

$$\varepsilon_6^{\perp}(k) = \left\{\left(\frac{D}{2} + b(\alpha_6)\left(K_0 - K(k)\right)\right)\times \times\left(\frac{D}{2} + b(\alpha_6)\left(K_0 + K(k) - 2J(k)\right)\right)\right\}^{1/2}. \quad (15)$$

The dependence of the excitation spectra on the temperature is determined by the terminal factors $b(\alpha_i)$. As in the FM phase, there are three branches of the SN phase, one of which (13) is a "longitudinal" and is related to the oscillation of the length of the magnetic moment vector, and the other two (14) and (15) are opposite and are related to the oscillations of a quadrupole ellipsoid.

Figure 4 shows the excitation spectra of a non-Heisenberg ferromagnet at different temperatures and different values of the anisotropy constant. As can be seen in Fig. 4 a–d, one of the transverse excitation branches ($\varepsilon_6^{\perp}$) is dispersionless at low temperatures and at arbitrary values of the anisotropy constant. However, with increasing temperature and anisotropy constants, this branch of excitations shows dependence on the wave vector, although it is not clearly expressed. This result can be understood if we take into account that the terminal multiplier $b(\alpha_6)$ is determined only by the excited energy levels E_0, E_{-1}, and therefore differs little from zero at arbitrary temperatures and values of the anisotropy constant D. The magnitude of the energy gap in this spectrum is determined by the anisotropy constant and increases significantly with the growth of D (see Fig. 4). The "transversal" branch ($\varepsilon_5^{\perp}$) has an energy gap, which significantly depends on the anisotropy constant. Besides, Fourier images of the exchange integrals K_0, J_0 also contribute to the gap. As can be seen in Fig. 4, this branch of excitations as a function of the wave vector behaves as $\sqrt{k^2 + a}$, and the temperature dependence is determined by the terminal factor $b(\alpha_2)$, i.e. the energy levels E_1 and E_0.

It should be noted that the "longitudinal" branch of the excitations $\varepsilon_4^{\parallel}$ is gap-free and, as follows from (13), should not depend on the anisotropy constant. However, as can be seen in Fig. 4, this branch, although weakly, still depends on anisotropy. This dependence is due to the influence of the q_2^2 tensor component of quadrupole moments (in the SN phase $q_2^2 = b(\alpha_2)$), which is associated with the anisotropy constant through the energy levels E_1 and E_{-1} of the magnetic ion (2), i.e. it is associated with the transition of the magnetic ion from the ground state to the most excited one.

4.3 Excitation spectra in the AFM phase at $T \neq 0$

Let's consider the behavior of excitation spectra in The AFM phase. In this phase, the exchange constants are connected by the ratio |J| > K, (J < 0) and the system can be divided into two equivalent sublattices. Since the sublattices are equivalent, it is sufficient to consider the spectra of the- one sublattice. As before, the spectra of elementary excitations are determined by the dispersion equation (6), which is valid at arbitrary temperatures and an arbitrary ratio of the material parameters of the system. The solution of equation (6) gives three branches of the magnon spectra, which have the form

$$\varepsilon_7^{\parallel} = b(\alpha_3)\times \times\left\{\left(2J_0 - K_0 - K(k)\right)\left(2J_0 - K_0 + K(k)\right)\right\}^{1/2}, \quad (16)$$

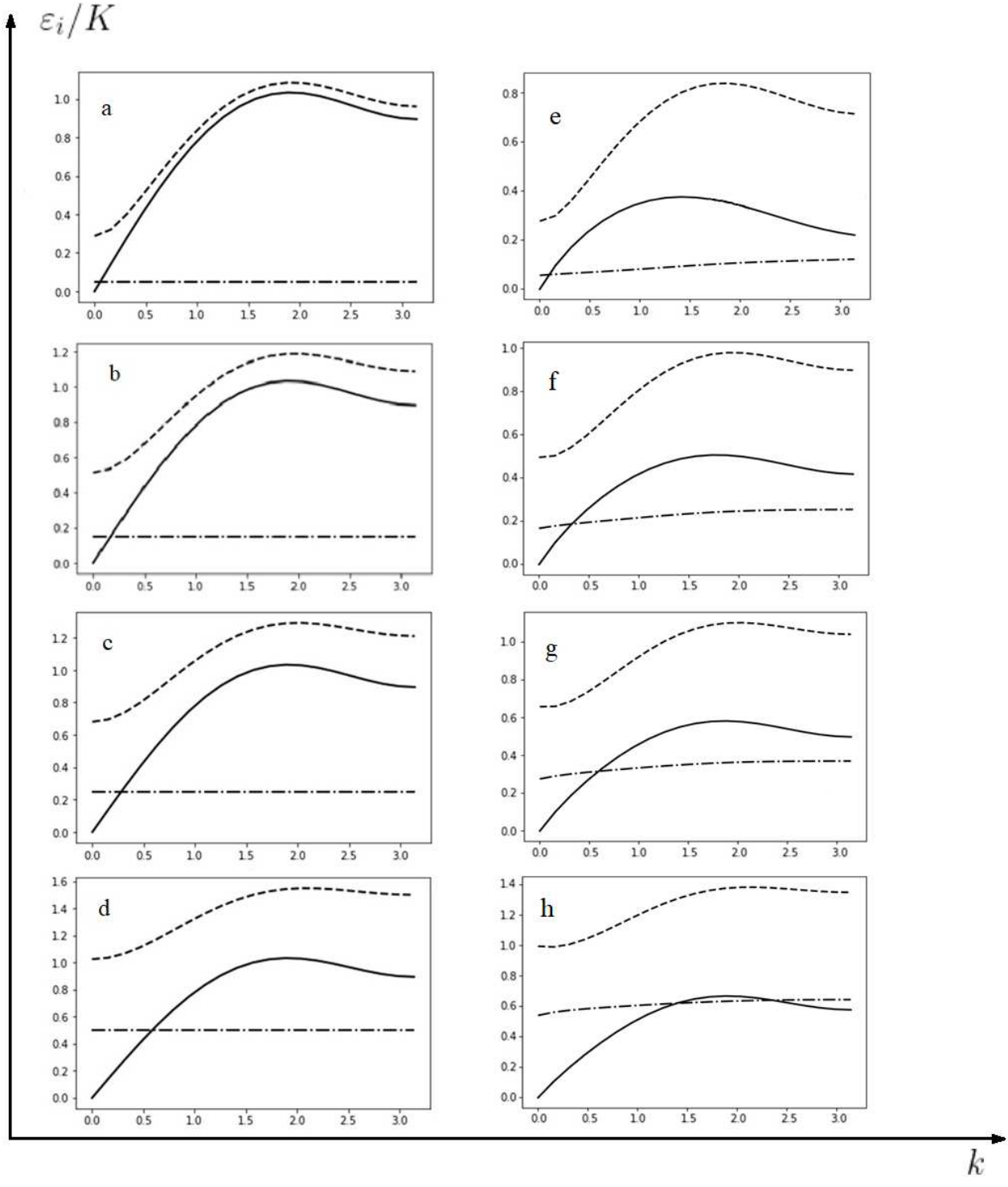

Fig. 4. The spectra of elementary excitations in a non-Heisenberg ferromagnet in SN phase at T/K = 0003 (a-d) and 0.4 (e-h) and the values of D/K = 0.1 (a, e), 0.3 (b, f), 0.5 (c, g), 1.0 (d, h). The solid lines correspond to the "longitudinal" branch of excitations $\hat{a}_4^{\parallel} / K$, dashed lines the "transversal" branch $\varepsilon_5^{\perp} / K$, and the dash-dotted "transversal" branch $\varepsilon_6^{\perp} /K$, the exchange integrals J = 0.2 K = 1.0.

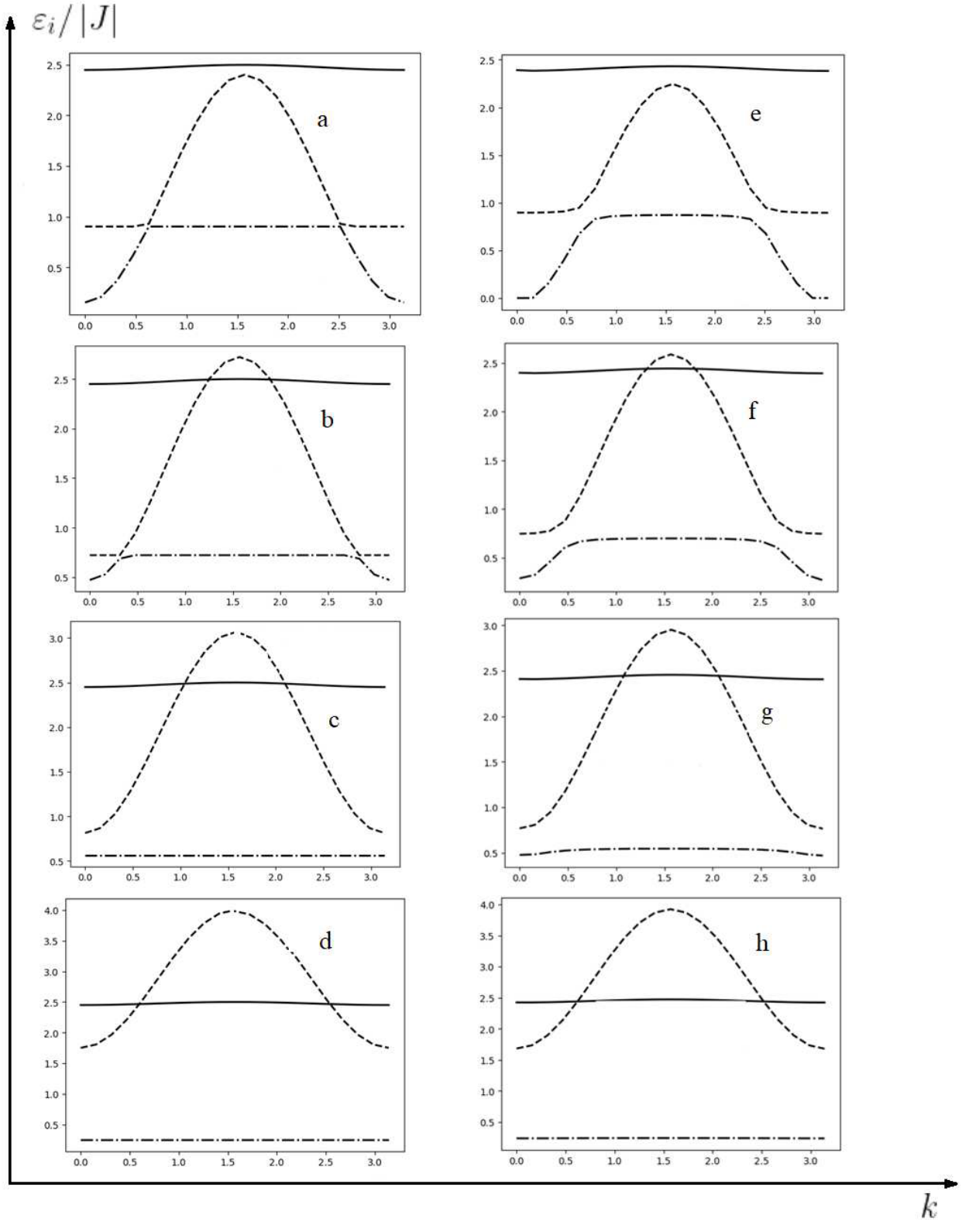

Fig. 5. Spectra of elementary excitations of a non-Heisenberg ferromagnet in the AFM phase at T/|J| = 0.003 (a-d) and 0.4 (e-h). D/|J| = 0.1 (a, e), 0.3 (b, f), 0.5 (c, g), 1.0 (d, h). Solid lines correspond to the "longitudinal" excitation branch $\varepsilon_7^{\parallel} / |J|$, dashed lines correspond to the "transversal" branch $\varepsilon_8^{\perp} / |J|$, and dashed lines correspond to the "transversal" branch $\varepsilon_9^{\perp} / |J|$, exchange intervals J = -1.0, K = 0.5.

$$\left(\varepsilon_{8,9}^{\perp}(k)\right)^2 = \frac{1}{2}\left[\begin{array}{c} E_{10}^2 + E_{0-1}^2 + 2\left(J(k)\right)^2 b(\alpha_1)b(\alpha_5) - \\ -\left(b^2(\alpha_1) + b^2(\alpha_5)\right)\left(J(k) - K(k)\right)^2 \end{array}\right] \pm \frac{1}{2}\sqrt{B}, \quad (17)$$

where

$$\begin{array}{c} B = \left(E_{10}^2 - E_{0-1}^2\right)^2 + \\ + 4\left(J(k)\right)^2 b(\alpha_1)b(\alpha_5)\left(E_{10} - E_{0-1}\right)^2 - \\ -2\left(J(k) - K(k)\right)^2\left(E_{10}^2 - E_{0-1}^2\right)\left(b^2(\alpha_1) - b^2(\alpha_5)\right) + \\ + \left[\begin{array}{c} \left(J(k) - K(k)\right)^2\left(b^2(\alpha_1) + b^2(\alpha_5)\right) - \\ -\left(J(k)\right)^2 b(\alpha_1)b(\alpha_5) \end{array}\right]^2 - \\ -4\left[\left(2J(k) - K(k)\right)K(k)b(\alpha_1)b(\alpha_5)\right]^2. \end{array} \quad (18)$$

In the ratios (16), (17) it is taken into account that in the AFM phase the parameters of the u-v transformation are equal to $\theta = 0$, $\theta = \pi/2$ for the first and second sublattices, respectively.

Let's analyze the received branches of the expectations. The branch of the $\varepsilon_7^{\parallel}(k)$ (see formula (17)) It is a longitudinal branch of excitations, i.e. it is associated with the transition of a magnetic ion from the ground state (E_1) to the most excited (E_{-1}) and with an oscillation of the length of the magnetic moment vector. As follows from Figure (16) and Fig. 5, this branch of excitations is symmetric with respect to $k = 0$ and $k = \pi$, moreover, the dependence on the wave vector is quite weak. In addition, this branch practically does not depend on temperature and the constant of single-ion anisotropy, and the energy gap in the spectrum of longitudinal excitations is determined by zero Fourier components of exchange integrals.

In addition to the "longitudinal" excitation branch, there are two "transversal" excitation branches in the AFM phase (see expression (17)). As follows from (17) and Fig. 5, these branches are "entangled", and with an increase in temperature and the anisotropy constant, this "entanglement" decreases and between the branches $\varepsilon_8^{\perp}$ and $\varepsilon_9^{\perp}$, there is a significant repulsion. Note that the excitation described by the $\varepsilon_8^{\perp}$ spectrum is associated with the transition of the magnetic ion from the basic state (E_1) to the first excited state (E_0). This branch of excitations has a fairly standard form for the AFM phase, and the energy gap in the $\varepsilon_8^{\perp}$ spectrum significantly depends on both temperature and the anisotropy constant. As for the $\varepsilon_9^{\perp}$ branch, it is associated with the transition of the magnetic ion from the first excited state (E_0) to the most excited state (E_{-1}). It is noteworthy that this excitation is not relaxation and has a number of features. Thus, at sufficiently low temperatures, this branch of excitations essentially depends on the wave vector (at low ($k \sim 0$) and large ($k \sim \pi$) wave vectors), and in the rest of the region of the wave vector is dispersion-free. With the growth of temperature and anisotropy, this branch becomes more and more dispersive throughout the entire range of wave vectors.

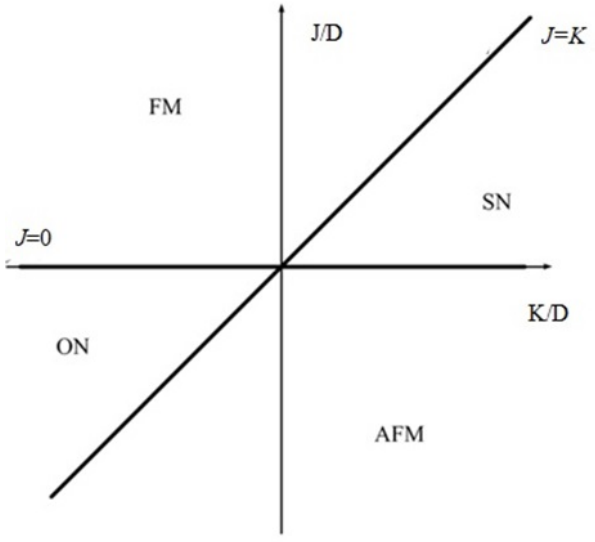

Fig. 6. Phase diagram of a non-Heisenberg anisotropic magnet with S = 1.

5. PHASE DIAGRAM

The conducted studies allow us to construct a cross-section of the phase diagram of a non-Heisenberg ferromagnet on the plane (J,K) at different-temperature values. As noted earlier, such a phase diagram was obtained for the system under study at $T = 0$ (see [26, 43]).

As is known, the phase transition line is determined from the condition of equality of thermodynamic potentials defined in the corresponding phases [13]. Thus, the phase transition lines FM-SN, SN–AFM, AFM–ON, ON–FM can be obtained from the condition of equality of free energies in the corresponding phases. Free energy is equal to $F = -T\ln Z$, where Z is the statistical sum in the corresponding phase, which is determined by the ratio

$$Z = \sum_{M=-1,0,1} \exp\left(-E_M / T\right).$$

Taking into account the ratios (2), (3)–(5) and (7), as well as the values of the u-v transformation parameters in the corresponding phases, numerical analysis allows us to construct a phase diagram at different values of the single-ionic anisotropy constant and free temperatures (excluding the fluctuation region).

So, from the equality of free energies in the FM and SN phases, we obtain a phase transition line between them:

$$J_0 = K_0. \tag{19}$$

Comparing the free energies in the phases SN and AFM, we obtain the phase transition line between them having the form

$$J_0 = 0. \tag{20}$$

If we compare the free energies in the phases of AFM and ON, we get a phase transition line between them in the form

$$\left|J_0\right| = \left|K_0\right|, \tag{21}$$

and from the equality of free energies in the ON and FM phases we obtain

$$J_0 = 0. \tag{22}$$

As follows from the relations (18)–(21), the phase diagram of a non-Heisenberg anisotropic magnet with S = 1 does not depend on either temperature or the value of the anisotropy constant and exactly coincides with the phase diagram of a similar system obtained earlier for the case T = 0 (see [26, 42]). An explicit view of the non-Heisenberg anisotropic magnet phase diagram with S = 1 is shown in Fig. 6.

It should be noted that the lines of phase transitions (18)-(21) can be determined by analyzing the excitation spectra in the corresponding phases. Thus, in the FM phase, the spectrum of longitudinal magnons loses stability (at k = 0) on the line $J_0 = K_0$ (see (10)). On the same line, the branch of "longitudinal" magnons in the SN phase loses stability (at k = π) (see (13)). Therefore, the line defined by the ratio (18) is the FM-SN phase transition line. At k = 0, the spectrum of three-dimensional magnons (13) in the SN phase on the line $J_0 = 0$ loses stability. Similarly, in the AFM phase, the spectrum of (16) "longitudinal" excitations becomes unstable at k = π on the line $J_0 = 0$, i.e. this line is the SN–AFM phase transition line. The same spectrum (16) loses stability at k = 0 on the line $\left|J_0\right| = \left|K_0\right|$, which indicates an AFM-ON phase transition. Moreover, the instability of the "longitudinal" branch of the disturbances (10) at k = π indicates that there is a phase transition on the line $\left|J_0\right| = 0$ | AM–ON.

The analysis of the phase diagram and the excitation spectra of a non-Heisenberg ferromagnet with anisotropy of the "light axis" type indicates that the FM-SN phase transition is a degenerate transition of the first kind.

6. CONCLUSION

The paper analyzes the dependence of the order parameters, free energy density and the spectra of elementary excitations on the temperature and the value of the constant of single-ion anisotropy of the type "light axis" of a non-Heisenberg anisotropic magnet with S = 1 and dimension d = 3 in the mean field approximation.

Numerical analysis of both vector and tensor order parameters in ferromagnetic, nematic, antiferromagnetic and orthogonal-nematic phases makes it possible to determine the temperature of transition to the paramagnetic state. In addition, the temperature dependence of the components of the quadrupole moment tensor q_2^0 (see Fig.1 a,..., l) indicates that at $T > T_Q$, i.e. in the paramagnetic phase, the rotational symmetry of the $Q_{\alpha\beta}$ tensor is also violated, which is due to the presence of a single-depth anisotropy of the type "light axis". Note that the transition temperatures significantly increase with the growth of the one-ion constant anisotropies of the type "light axis" (see Fig. 1), which is quite expected, since a large light-axial anisotropy prevents the destruction of the magnetic order by thermal fluctuations. Also, in the mean field approximation, we carried out an analytical assessment of the temperatures of transitions to a more symmetrical phase from both phases with a vector parameter of order (FM, AFM) and phases characterized by tensor parameters (SN and ON). These estimates show that the transition temperatures significantly depend on tensor order parameters and biquadratic exchange interaction.

Of particular interest is the dependence of the spectra of elementary excitations of a non- Heisenberg anisotropic ferromagnetic with a spin of a magnetic ion unit on both temperature and the anisotropy constant. First of all, we note that, unlike the previously considered case, T = 0 [43], in the case under consideration, an additional branch of excitations arises associated with the transition of the magnetic ion from the first excited state of the magnetic ion (E_0) to the most excited (E_{-1}), and this branch is not relaxation. Thus, in the

non-Heisenberg magnetism at arbitrary temperatures (below the critical temperature), three branches of elementary disturbances are realized: two of which are transversal and are associated with the precession motion of a quadrupole ellipsoid, and one is transversal, associated with a change in the length of the magnetic moment vector. The behavior of the excitation spectra in dipole and tensor phases is fundamentally different. Thus, in the FM and AFM phases, the transversal branches of the excitation at low values of the light-axial anisotropy constant and sufficiently low temperatures are strongly hybridized (see Fig. 3 and 5) and significantly depend on the magnitude of the anisotropy. With an increase in the anisotropy constant, the "transversal" branches begin to push apart, and at high values of the single-ion anisotropy constant, the transverse branches associated with the transition of the magnetic ion E_{0-1} become dispersionless. In the SN phase, the "transversal" branches of elementary disturbances are not hybridized, which is due to the equality of the average value of the magnetic moment to zero (at the node). In addition, in this phase, taking into account single-ion anisotropy removes the degeneration of the excitation branches, as is observed, for example, in an isotropic spin nematic [26].

The analysis of the free energy density and the spectra of "longitudinal" excitations makes it possible to construct a phase diagram of the system under study at arbitrary temperatures and arbitrary values of the single-ionic anisotropy constant. The result of these studies is shown in Fig. 6. As shown in this figure, the system retains the same phase states that are realized at T = 0. In addition, the phase transition lines are similar to the case T = 0, i.e. they do not depend on either temperature or the value of the anisotropy constant. Thus, the phase diagram we obtained coincided with the phase diagram of the system under study at T = 0 [53]. In addition, the phase transition in the case under consideration is a degenerate phase transition of the first kind, as well as at T = 0. However, this does not mean at all that temperature and single-ion anisotropy do not affect the properties of the spin nematic. As shown in this paper, temperature and single-ion anisotropy fundamentally change the dynamic properties of the system.

It should also be noted that the analysis of the spectra of elementary disturbances in the ON-phase has not been carried out in this work. This is the subject of a separate review.

FUNDING

The work was carried out with the support of the Russian Science Foundation (grant No. 23-22-00054).

REFERENCES

1. E. G. Galkina, B. A. Ivanov LOW TEMPERATURE PHYSICS, **44,** 618 (2018) https://doi.org/10.1063/1.5041427
2. V.G. Bar'yakhtar, B.A. Ivanov, M.V. Chetkin Soviet Physics Uspekhi, 28, 563 (1985) **DOI** 10.1070/PU1985v028n07ABEH003871
3. B. A. Ivanov and D. D. Sheka, Phys. Rev. Lett. 72, 404 (1994)
4. E. G. Galkina, B. A. Ivanov JETP Lett, **61**, 511 (1995)
5. H. V. Gomonay and V. M. Loktev, Phys. Rev. B 81, 144427 (2010), https://doi.org/10.1103/PhysRevB.81.144427
6. O. A. Tretiakov, D. Clarke, G.-W. Chern, Y .B. Bazaliy, and O. Tchernyshyov, Phys. Rev. Lett. 100, 127204 (2008), https://doi.org/10.1103/PhysRevLett.100.127204
7. E. G. Galkina, B. A. Ivanov, S. Savel'ev, and F. Nori, Phys. Rev. B 77, 134425 (2008), https://doi.org/10.1103/PhysRevB.77.134425
8. O. Gomonay, T. Jungwirth, and J. Sinova, Phys. Rev. Lett. 117, 017202 (2016), https://doi.org/10.1103/PhysRevLett.117.017202
9. E. G. Galkina, B. A. Ivanov, Low Temp. Phys. 44, 618 (2018), https://doi.org/10.1063/1.5041427
10. R. Cheng, D. Xiao, and A. Brataas, Phys. Rev. Lett. 116, 207603 (2016), https://doi.org/10.1103/PhysRevLett.116.207603
11. R. Khymyn, I. Lisenkov, V. Tyberkevych, B. A. Ivanov and A. Slavin, Sci. Rep. 7, 43705 (2017), https://doi.org/10.1038/srep43705
12. R. V. Ovcharov, E. G. Galkina, B. A. Ivanov, and R. S. Khymyn, Phys. Rev. Appl. 18, 024047 (2022), https://doi.org/10.1103/PhysRevApplied.18.024047
13. L.D.Landau and E.M.Lifshitz Electrodynamics of Continuous Media, V.8 of Course of Theoretical Physics, Pergamon Press, 1984
14. A.F. Andreev , V.I. Marchenko,Sov. Phys. Usp. **23** 21(1980) DOI: 10.1070/PU1980v023n01ABEH004859
15. A. F. Andreev and I. A. Grishchuk, Sov. Phys. JETP 60, 267 (1984).
16. R. Okazaki, T. Shibauchi, H. J. Shi, Y. Haga, T. D. Matsuda, E. Yamamoto, Y. Onuki, H. Ikeda, and Y. Matsuda, Science 331, 439 (2011), https://doi.org/10.1126/science.1197358.
17. S. Kasahara, T. Shibauchi, K. Hashimoto, K. Ikada, S. Tonegawa, R. Okazaki, H. Shishido, H. Ikeda, H. Takeya, K. Hirata, T. Terashima, and Y. Matsuda, Phys. Rev. B 81, 184519 (2010), https://doi.org/10.1103/PhysRevB.81.184519

18. R. Fernandes, A. Chubukov, and J. Schmalian, Nat. Phys. 10, 97 (2014), https://doi.org/10.1038/nphys2877

19. S. Kasahara, H. J. Shi, K. Hashimoto, S. Tonegawa, Y. Mizukami, T. Shibauchi, K. Sugimoto, T. Fukuda, T. Terashima, A. H. Nevidomskyy, and Y. Matsuda, Nature (London) 486, 382 (2012), https://doi.org/10.1038/nature11178

20. X. Lu, J. Park, R. Zhang, H. Luo, A. H. Nevidomskyy, Q. Si, and P. Dai, Science 345, 657 (2014), https://doi.org/10.1126/science.1251853

21. A. E. Bohmer and A. Kreisel, J. Phys.: Condens. Matt. 30, 023001 (2018), https://doi.org/10.1088/1361-648X/aa9caa

22. A.M.Perelomov, Sov. Phys. Usp. 20, 703 (1977), https://doi.org/10.1070/PU1977 v020n09ABEH005459

23. A. Perelomov, Generalized Coherent States and Their Applications, Springer-Verlag, Berlin (1986).

24. B. A. Ivanov and A. K. Kolezhuk, Phys. Rev. B 68, 052401 (2003), https://doi.org/10.1103/PhysRevB.68.052401

25. N. Papanikolaou, Nucl. Phys. B 305, 367 (1988).

26. Yu. A. Fridman, O. A. Kosmachev, and Ph. N. Klevets, JMMM 325, 125 (2013), http://dx.doi.org/10.1016/j.jmmm.2012.08.027

27. A. Lauchli, F. Mila, and K. Penc, Phys. Rev. Lett. 97, 087205 (2006), https://doi.org/10.1103/PhysRevLett.97.229901

28. A. Smerald and N. Shannon, Phys. Rev. B 88, 184430 (2013), https://doi.org/10.1103/PhysRevB.88.184430

29. G. Fath and J. Solyom, Phys. Rev. B 44, 11836 (1991), https://doi.org/10.1103/PhysRevB.44.11836

30. A. A. Zvyagin and V. V. Slavin, Phys. Rev. B 106, 054429 (2022), https://doi.org/10.1103/PhysRevB.106.054429

31. Yu.A. Fridman. O.A. Kosmachev, A. K. Kolezhuk, and B.A. Ivanov, Phys. Rev. Lett. 106, 097202 (2011), https://doi.org/10.1103/PhysRevLett.106.097202

32. O. A. Kosmachev, Yu. A. Fridman, E. G. Galkina, and B. A. Ivanov, JETP 120, 281 (2015), https://doi.org/10.7868/S0044451015020121

33. L. E. Svistov, T. Fujita, H. Yamaguchi, S. Kimura, K. Omura, A. Prokofiev, A. I. Smirnov, and Z. Honda, M. Hagiwara, JETP Lett. 93, 2 (2011).

34. P. G. de Gennes. Physics of liquid crystals. Clarendon press. Oxford 1974

35. M. E. Zhitomirsky and H. Tsunetsugu, Europhys. Lett. 92, 37001 (2010), https://doi.org/ 10.1209/0295-5075/92/37001

36. C. L.Ginzburg, Fizika Tverdogo Tela **12**, 1805 (1970).

37. Y. Y. Hsieh and M. Blume, Phys. Rev. B 8, 2684 (1972), https://doi.org/10.1063/1.1853192

38. E. L. Nagaev, Magnets with complex exchange interactions, Nauka, Moscow, 1988

39. V. M. Matveev, Sov. Phys. JETP 38, 81 (1974).

40. Yu. A. Fridman and D.V.Spirin, Phys. Stat. Sol. (b) 231, 165 (2002), https://doi.org/10.1002/1521-3951(200205)

41. D. V. Spirin and Yu. A. Fridman, J. Magn. Magn. Mater. 260, 215 (2003).

42. A. V. Chubukov, J. Phys. Cond. Matt. 2, 1593 (1990).

43. E. A. Yarygina, Ya. Yu. Matyunina, Ph. N. Klevets, and Yu. A. Fridman, J. Magn. Magn. Mater. 167043 (2020), https://doi.org/10.1016/j.jmmm.2020.167043

44. Yu. N. Mitsai and Yu. A. Fridman, TMF 81, 263 (1989)

45. V. V. Val'kov, Sov. J. Theor. Math. Phys. 76, 766 (1988), https://doi.org/10. 1134/S1063783412070128

46. Yu. A. Fridman, O. A. Kosmachev, and Ph. N. Klevets, J. Magn. Magn. Mater. 320, 435 (2008). doi:10.1016/j.jmmm.2007.07.001

47. R.O.Zaitsev, Sov. JETP, **41**, 100 (1975).

48. Yu.A. Izyumov, F. A. Kassan-Ogly, Yu.N. Skryabin, Field methods in the theory of ferromagnetism, Nauka, Moscow, 1974.

49. V. G. Baryakhtar, V. N. Krivoruchko, D. A. Yablonsky, Green's functions in the theory of magnetism, Nauk. Dumka, Kyiv, 1984.

50. Yu. A. Fridman and O. A. Kosmachev, Phys. Sol. St. 51, 1167 (2009), https://doi.org/10.1134/S1063783409060146

51. V. V. Val'kov, T. A. Val'kova, and S. G. Ovchinnikov, JETP 88, 550 (1985).

52. V.V. Valkov, S. G. Ovchinnikov, Quasiparticles in strongly correlated systems, Publishing house SB RAS, Novosibirsk, 2001.

53. E. A. Yaryginaa, Ya. Yu. Matyuninaa, Ph. N. Klevetsa, and Yu. A. Fridman, JETP 129, 1070 (2019), https://doi.org/10.1134/S1063776119110086

54. V. I. Butrim, B. A. Ivanov, O. A. Kosmachev, and Yu. A. Fridman, Phys. Sol. St. 54, 1363 (2012).

55. V. I. Butrim, B. A. Ivanov, and Yu. A. Fridman, Low Temp. Phys. 38, 395 (2012), http://dx.doi.org/10.1063/1.4709439

56. O. A. Kosmachev, Yu. A. Fridman, and B. A. Ivanov, JETP Lett. 105, 453 (2017), https://doi.org/10.1134/S0021364017070086